Asian Journal of Atmospheric Environment
Vol. 5-2, pp.79-85, June 2011
doi: 10.5572/ajae.2011.5.2.079

Sensitivity Analysis by Using Global Imager for Retrieval of Biomass Burning Aerosols

Hyun Jin Lee and Jae Hwan Kim*

Department of Atmospheric Science, Pusan National University, Geumjeong-gu, Busan 609-735, Korea

*Corresponding author. Tel: +82-51-510-2172, E-mail: jaekim@pusan.ac.kr

ABSTRACT

The purpose of this study is to evaluate the strength of the near-UV wavelength of 380 nm relative to visible and near-IR bands, and to find the suitable wavelength for detecting aerosols by using the Global Imager (GLI) sensor aboard the Advanced Earth Observing Satellite-II (ADEOS-II). Sensitivity analysis is performed for the retrieval of biomass burning aerosols by employing the radiative transfer model Rstar5b. It is determined that background surface reflectance in the blue band is similar to that in the near-UV band, and that wavelengths in the blue bands are more sensitive to the Aerosol Optical Thickness (AOT) than wavelengths in the near-UV band. The Total Ozone Mapping Spectrometer (TOMS) Aerosol Index (AI) is used in the indirect method used for aerosol retrieval, and the wavelength pair 380 nm and 460 nm is determined to be the most sensitive to the AOT. The results of this study suggest that wavelengths in the blue bands are suitable for detecting biomass burning aerosols over the Korean peninsula.

Key words: Biomass burning aerosols, Global Imager, Blue band, Near-UV, Rstar5b

1. INTRODUCTION

Tropospheric aerosols are important not only because they are air pollutants, but also because they control the global energy budget through direct and indirect radiative forcing (Alpert *et al*., 1998; Miller and Tegen, 1998; Schwartz *et al*., 1995). However, the effect of aerosols includes the uncertainty in global climate (Solomon *et al*., 2007). National Aeronautics and Space Administration (NASA) operates the Aerosol Robotic NETwork (AERONET), which is a ground-based aerosol monitoring system that estimates aerosol properties such as refractive index and size distribution (Dubovik *et al*., 2000; Holben *et al*., 1998). However, satellite measurements are also valuable since they provide high temporal and spatial coverage of the globe, and since aerosols are distributed over a wide area and can be transported to other areas by prevailing winds.

Methods for detecting aerosols using satellite measurements are broadly categorized as direct or indirect methods of aerosol retrieval. The direct method involves the retrieval of the Aerosol Optical Thickness (AOT), while the indirect method involves the retrieval of the aerosol index with a multi-wavelength ratio using satellite measurements. Satellite Aerosol retrieval requires a detailed sensitivity analysis of aerosols with respect to wavelengths, because scattering and absorption by aerosols depend strongly on the wavelength. IR bands have the advantage that they can be used to detect aerosol signals at nighttime, but aerosol retrieval using IR bands is applicable only to the case of large aerosols when water vapor information is available. The Visible and Short Wave Infrared (SWIR) band has been widely used for aerosol retrieval. However, the band has the disadvantage that no significant radiation change is observed in a restricted area with highly reflective surfaces despite the presence of aerosols. This disadvantage hampers aerosol retrieval as well as cloud retrieval over snow-covered surfaces. The advantage of using the near-UV band to detect aerosols is that the surface reflectance is low in this band even in the case of highly reflective surfaces such as those in deserts. In addition, it is not influenced by the aerosol phase function, and the effect of the Bidirectional Reflectance Distribution Function (BRDF) on this band is weak (Torres *et al*., 2002). Even though there have been many studies on sensitivity tests for various wavelengths to examine the suitability of these wavelengths for detecting aerosols, few studies have focused on sensitivity analyses of different bands, including both UV and visible bands with high spatial resolution. The Global Imager (GLI) provides the best data set for this kind of study, because it covers bands ranging from shortwave UV to thermal IR.

In this study, we analyzed the suitability of various bands of different wavelengths for detecting aerosols, and used data from GLI for our analysis. The GLI has several unique wavelength bands from near-UV to thermal-IR, with a spatial resolution ranging from 250 m to 1 km at the nadir, which is similar to the resolution of the Moderate Resolution Imaging Spectroradiometer (MODIS). The GLI was operational only for a short period from December 2002 to October 2003. The Second-Generation Global Imager (SGLI) is scheduled to be launched in 2013 as part of the Advanced Earth Observing Satellite-II (ADEOS-II) mission. Therefore, this sensitivity analysis provides information that will be useful in employing SGLI for aerosol retrieval and in obtaining the characteristics of aerosols over East Asia.

On the basis of the results of the sensitivity analysis, we determined the GLI measurement that was suitable for direct aerosol retrieval. A pair of wavelengths was found to be suitable for direct and indirect aerosol retrieval. We performed direct and indirect aerosol retrieval for a specific case.

2. DATA AND RADIATIVE TRANSFER MODEL (RTM)

In order to find a wavelength suitable for detecting aerosols, we evaluated 12 wavelengths out of the 36 wavelengths of GLI measurements: 380 nm, 400 nm, 412 nm, 443 nm, 460 nm, 490 nm, 545 nm, 679 nm, 760 nm, 865 nm, 1,136 nm, and 2,100 nm (between near-UV and SWIR bands). The wavelength used at present in the satellite retrieval algorithm for the aerosol retrieval was also evaluated. Even though the spatial resolutions at the nadir were either 250 m or 1 km depending on the wavelength, the GLI data were regridded onto a $0.1° \times 0.1°$ grid to reduce the random error resulting from the noise in each pixel.

In this study, we utilized the Radiative Transfer Model (RTM) Rstar5b for the sensitivity analysis of wavelengths. Rstar5b has advantages such as easy data control and short computing time when used to perform simulations. It is a general package to simulate radiation fields in the atmosphere-land-ocean system at wavelengths between 0.2 μm and 200 μm, and it was developed by T. Nakajima and his group at Tokyo University (Nakajima *et al.*, 2003; Nakajima and Tanaka, 1988; Nakajima and Tanaka, 1986). Rstar5b has 11 aerosol databases with 9 fundamental materials information (Table 1).

Table 1. The database of aerosol parameters in Rstar5b.

No.	Model name	Particle matter	Mixing ratio
1	Water	Water	1.0
2	Ice	Ice	1.0
3	Dust-like	Dust-like	1.0
4	Soot	Soot	1.0
5	Volcanic-ash	Volcanic-ash	1.0
6	75% H_2SO_4	75% H_2SO_4	1.0
7	Rural	Water-soluble, Dust-like	0.7 : 0.3
8	Sea spray	Sea salt	1.0
9	Urban	Water-soluble, Dust-like, Soot	0.56 : 0.24
10	Tropo	Water-soluble, Dust-like	0.7 : 0.3
11	Yellow sand	Yellow sand	1.0

Taken from d'Almeida *et al.*, 1991

3. METHODOLOGY

In the sensitivity analysis of each wavelength, the increment in the amount of aerosols was determined based on the variation of aerosol reflectance, which was calculated as follows.

In the case of a clear sky, the reflectance at the top of the atmosphere (Rt) comprises the background surface reflectance (Rs), the Rayleigh reflectance (Rr), and the aerosol reflectance (Ra) (Higurashi and Nakajima, 1999; Gordon and Wang, 1992). Thus, the aerosol reflectance can be expressed by the following equation:

$$Ra = Rt - Rr - Rs \cdot tt \quad (1)$$

where *tt* is the transmittance between the surface and the atmosphere. Rt represents the reflectance measured by a satellite, and Rr was calculated by using the RTM. However, it is impossible to determine the background surface reflectance in the presence of aerosols. The minimum reflectance method was adopted by Hauser *et al.* (2004) to determine the background surface reflectance. In this method, the lowest value of the calculated surface reflectance over a certain period of time is considered to be the background surface reflectance. In this study, the background surface reflectance was determined on the basis of the calculated surface reflectance over 30 days. This period, which is shorter than that considered by Hauser *et al.* (2004), was considered because the surface reflectance changes due to the growth of vegetation during spring in the month of May.

To reduce errors, the calculated surface reflectances for all wavelengths over the areas with over 8% reflectance at 380 nm were neglected while calculating the background surface reflectance, as described by Herman and Celarier (1997). They suggest that the background surface reflectances at 380 nm were lower than 8% in the area, including desert and ice-covered regions. For the cloud mask, we utilize the ratio of reflectance from 865 nm to 660 nm, which is part of the GLI Cloud Mask algorithm.

We performed the sensitivity analysis using the calculated theoretical aerosol reflectance on the basis of the calculated background surface reflectance, and aerosol retrieval was carried out by the direct and indirect methods.

In the case of indirect aerosol retrieval, the Total Ozone Mapping Spectrometer (TOMS) Aerosol Index (AI) adopted by Torres *et al.* (1998) was used. The AI depends on a spectral contrast because of the wavelength-dependent effects of aerosols. Positive values of the AI indicate the presence of absorbing aerosols such as mineral dust, carbonaceous aerosols, and biomass burning aerosols. We obtained the TOMS AI using the results of the GLI in the visible band by applying the following formula:

$$AI = -100\{\log_{10}(I_{\lambda 1}/I_{\lambda 2})_{meas} - \log_{10}[(I_{\lambda 1(Rs\lambda 1)}/I_{\lambda 2(Rs\lambda 2)})_{calc}]\} \quad (2)$$

where I_{meas} is the measured reflectance at two wavelengths ($I_{\lambda 1} < I_{\lambda 2}$) of GLI, I_{calc} is the calculated Rayleigh reflectance obtained by using RTM, and Rs is the background surface reflectance. The background surface reflectance remained constant in the near-UV bands; therefore, the background surface reflectance was not used to calculate the TOMS AI. In contrast, the GLI AI was composed of the visible and near-UV bands; therefore, the Rayleigh reflectance calculated using AI in this study includes the surface reflectance.

Because of industrial development and desertification in China, interest in aerosols over East Asia has recently grown (King *et al.*, 1999; Herman *et al.*, 1997). In fact, the biomass burning emissions in 2003 were more than twice the average annual emissions from Russian fires that occurred in 1996-2003 (Jaffe *et al.*, 2004). Lee *et al.* (2005) and In *et al.* (2008) showed that a biomass burning plume that covered northern China and the Korean peninsula was transported from Russia in May 2003; the plume significantly affected the regional environment. Therefore, in this study, we focused on the analysis of biomass burning aerosols in May 2003.

Rstar5b has 11 databases of aerosol parameters; however, data on biomass burning aerosols were unavailable. To perform sensitivity analysis of biomass burning aerosols, a database for biomass burning aerosols was calculated by using the aerosol properties observed at the AERONET sites in Beijing (China), Shirahama (Japan), Noto (Japan), Anmon (Korea), and Gosan (Korea).

4. RESULTS AND DISCUSSION

We calculated the background surface reflectance at the 12 wavelengths by using the GLI data obtained for May 2003 (data not shown). The calculated background surface reflectance varied with the surface characteristics over the Korean peninsula. Values were low over the mountainous area on the eastern side of the Korean peninsula. For a detailed analysis of the background surface reflectance, we evaluated the average of the background surface reflectances (shown in Fig. 1) over a vegetation area (128°E−130°E, 36°N−38°N).

Fig. 1 shows the calculated background surface reflectance as a function of wavelength. The background surface reflectances of long wavelengths increase slightly, and a peak is observed at 1,136 nm. This pattern of background surface reflectance is consistent with that observed by Kaufman and Tanre (1992) and Soufflet *et al.* (1997). Near-UV bands have an advan-

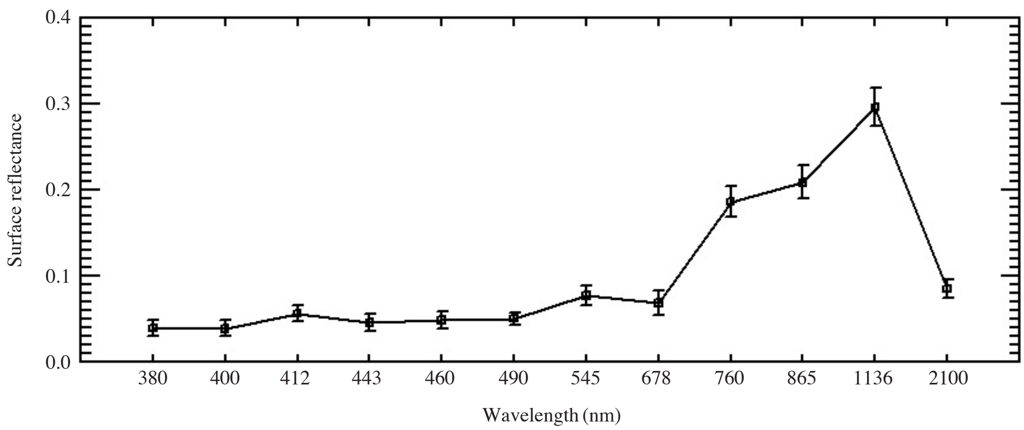

Fig. 1. Calculated background surface reflectance as a function of wavelength.

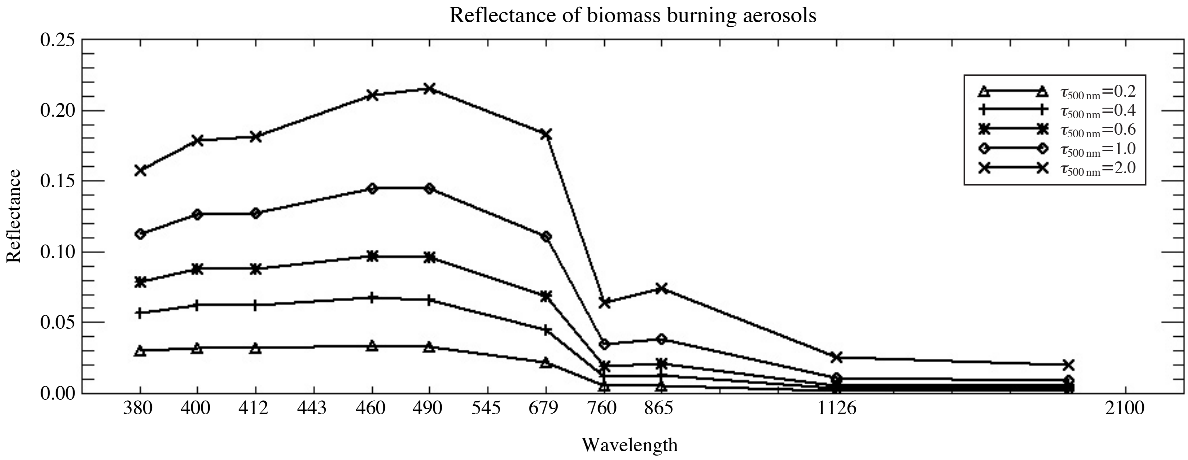

Fig. 2. Theoretical reflectance of biomass burning aerosols obtained by using Rstar5b (similar to Fig. 1).

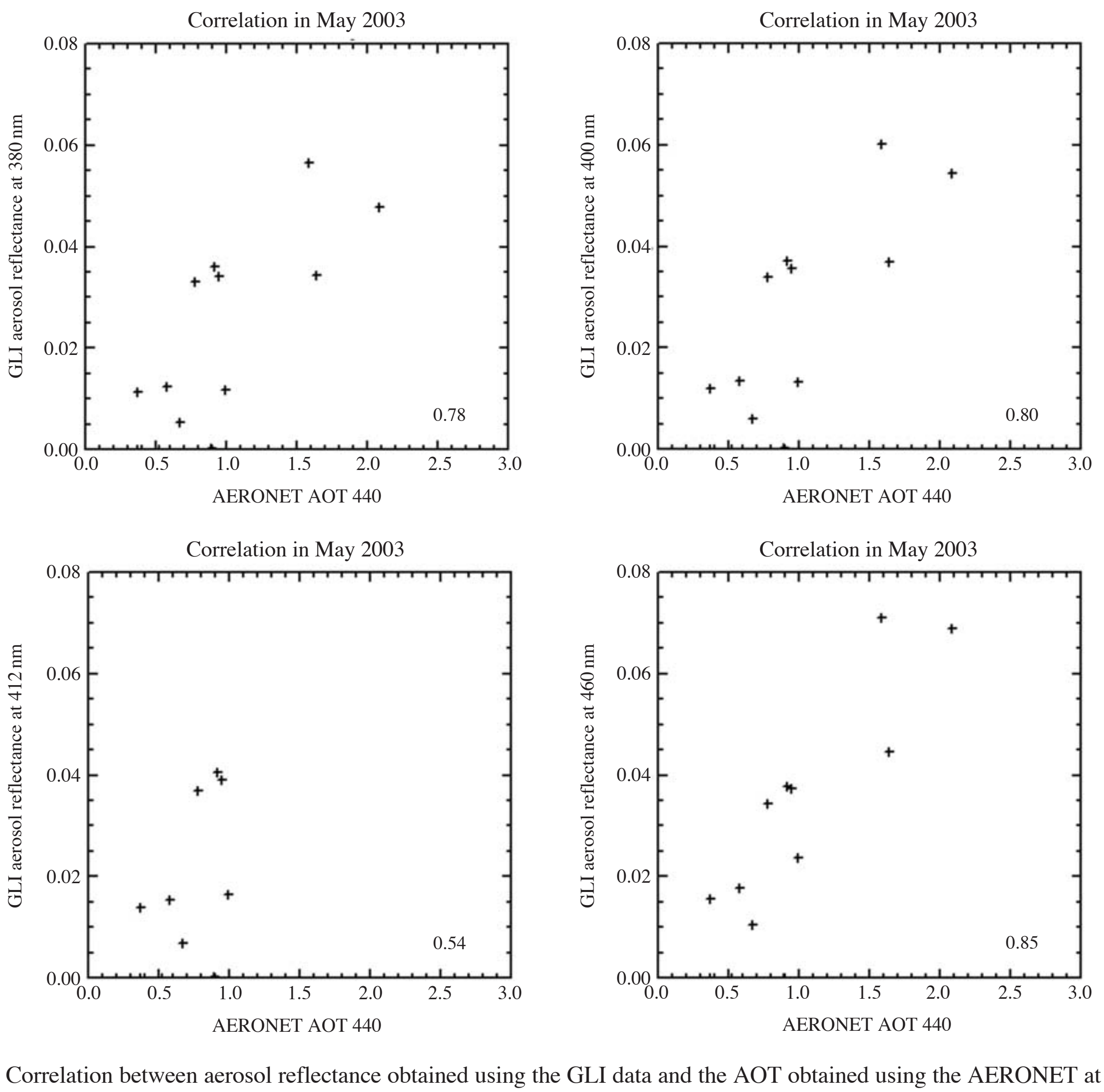

Fig. 3. Correlation between aerosol reflectance obtained using the GLI data and the AOT obtained using the AERONET at wavelengths of 380 nm, 400 nm, 412 nm, and 460 nm for May 2003. The number means a correlation coefficient between AOT and aerosol reflectance obtained using the GLI data.

tage in detecting aerosols due to their low surface reflectance (Torres *et al.*, 2002). As shown in Fig. 1, over the Korean peninsula, the background surface reflectance at 490 nm (i.e., in the blue band of visible) was not significantly different from that at 380 nm (i.e., in the near-UV band).

Fig. 2 shows the theoretical reflectance of biomass burning aerosols with background surface reflectance based on Fig. 1. Two wavelengths (443 nm and 545 nm) are eliminated in this analysis because surface reflectance of 443 nm is similar to that of 412 nm, and 545 nm shows a relatively high surface reflectance. The aerosol reflectance increases with aerosol except for 760 nm. Aerosol reflectance at a wavelength of 760 nm is very low compared to other wavelengths. The results showed that a wavelength of 760 nm is unsuitable for detecting biomass burning aerosols. The wavelengths from 380 nm to 490 nm are sensitive to increases in the AOT. In particular, wavelengths in the visible light band are more sensitive to increases in the AOT than wavelengths in the near-UV band.

As a result, we examined the capability of wavelengths for detecting aerosols, comparing aerosol reflectance from satellite measurement with in-situ AOT from AERONET. We utilized the wavelengths from 380 nm to 490 nm (5 of the 12 wavelengths), which are sensitive to the increase in the AOT. However, GLI is easily saturated in the presence of the clouds and aerosols due to concentrated reflectance of solar radiation in the case of the 490 nm wavelength. Therefore, we analyzed the suitability of the wavelengths 380 nm, 400 nm, 412 nm, and 460 nm for detecting aerosol signals. Fig. 3 shows the correlation between the aerosol reflectance obtained using GLI and the AOT values obtained from AERONET at the wavelengths of 380 nm, 400 nm, 412 nm, and 460 nm for May 2003. The correlation values range from 0.54 to 0.85. In particular, 460 nm shows the highest correlation for the value 0.85, and 412 nm shows the lowest correlation for the value 0.54. According to Fig. 1, surface reflectance at a wavelength of 412 nm is higher than those at the other wavelengths. This result illustrates that the correlation between the GLI aerosol reflectance and the AERONET AOT is relatively high with low surface reflectance for the selected wavelengths. This observation (i.e., it is difficult to detect aerosol signals as the surface reflectance increases) is consistent with those of previous studies (von Hoyningen *et al.*, 2003; Torres *et al.*, 2002; King *et al.*, 1999). These results indicate that the blue band is effective for detecting biomass burning aerosols over the Korean peninsula.

From this analysis we retrieve the AOT for the case of the 460 nm wavelength. Fig. 4 shows the AOT over

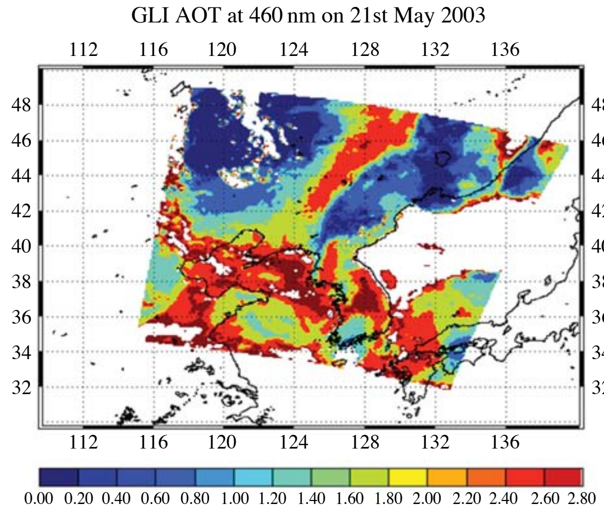

Fig. 4. AOT obtained from the GLI data on May 21, 2003 at a wavelength of 460 nm.

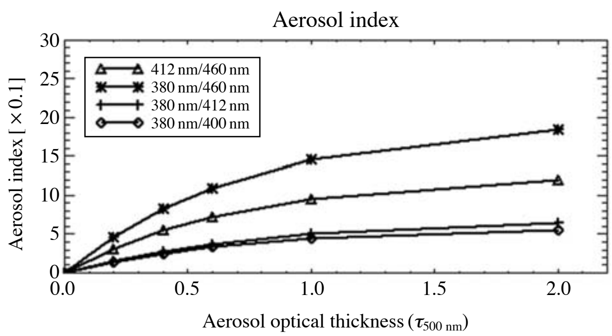

Fig. 5. The theoretical AI of biomass burning aerosols obtained by using the Rstar5b with background surface reflectance presented in Fig. 1.

the Korean peninsula on May 21, 2003. The biomass burning aerosols cover the Korean peninsula and China, and AOT is also high.

In addition, we simulated the theoretical GLI AI as part of the indirect method of aerosol retrieval (Fig. 5). The biomass burning aerosols retrieved using the GLI AI represent the absorption aerosols as TOMS AI. It was expected that the GLI AI with the wavelength pair 380 nm and 400 nm would be suitable for detecting biomass burning aerosols due to low surface reflectance and the similar characteristics of the two wavelengths. However, the results of the sensitivity analysis were not as expected. The variation in the GLI AI with the pair of 380 nm and 460 nm as the AOT increased was double that for 380 nm and 400 nm. This result indicates that the pair of 380 nm and 460 nm is appropriate for detecting biomass burning aerosols because of the suitability of the 460 nm wave-

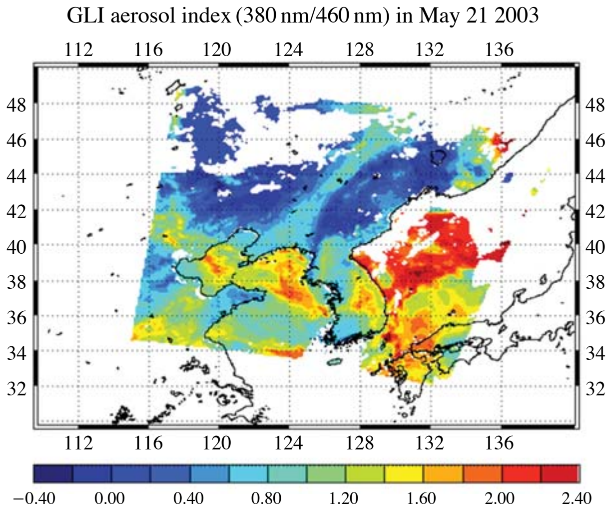

Fig. 6. The GLI AI for the wavelength pair of 380 nm and 460 nm.

length in detecting biomass burning aerosols.

Furthermore, Fig. 5 shows that the GLI AI is sensitive to the AOT for AOT values of 1.0 or less. However, the increase in the GLI does not change significantly when the AOT is greater than 1.0. This result suggests that it is difficult to retrieve the AOT by using GLI AI when the concentration of aerosol is high.

Based on this analysis, the GLI AI with the pair of 380 nm and 460 nm is retrieved. Fig. 6 shows the AI over the Korean peninsula on May 21, 2003. The pattern of AI is similar to that of AOT as shown in Fig. 4. The GLI AI values range from 0.6 to 2.0 over the presence of biomass burning aerosols, as shown in Fig. 4. The error is about 1.0 between the AOT retrieved using sensitivity analysis of Fig. 5 and the AOT retrieved using the wavelength of 460 nm in Fig. 4. This result also suggests that it is difficult to retrieve the AOT by using GLI AI when the concentration of aerosol is high.

5. CONCLUSIONS

Near-UV bands can be used to detect aerosols because of their low surface reflectance. However, in this study we observed that the background surface reflectance in the blue band of visible light is the same as that in the near-UV band over the Korean peninsula. In addition, the visible bands are more sensitive to the AOT than the near-UV bands are. On the basis of these results, we suggest that the blue band is suitable for detecting biomass burning aerosols over the Korean peninsula. By applying the TOMS AI in the GLI measurements, the GLI AI for the pair of 380 nm and 460 nm is found to be better than that for the pair of 380 nm and 400 nm for detecting the signals of biomass burning aerosols. We conclude that a wavelength of the blue band is suitable for detecting biomass burning aerosols over the Korean peninsula, and can be used for the SGLI aboard GCOM-C1.

The sensitivity analysis used in this study is specifically applicable to the case of biomass burning aerosols. Further study is required to analyze other aerosols because these results are strongly dependent on the aerosol properties. On the basis of these studies, it will be possible to develop a highly accurate algorithm for aerosol retrieval.

ACKNOWLEDGEMENTS

The authors are grateful to the Japan Aerospace Exploration Agency (JAXA) for providing the GLI data and OpenCLASTR project for using RSTAR (system for transfer of atmospheric radiation package in this study). This work was supported by the Research Agency for Climate Science funded by the Korea Meteorological Administration (RACS 2010-1011).

REFERENCES

Alpert, P., Kaufman, Y.J., Shay-EL, Y., Tanré, D., Da Silva, A., Joseph, Y.H. (1998) Quantification of dust-forced heating of the lower troposphere. Nature 395, 367-370.

d'Almeida, G.A., Koepke, P., Shettle, E.P. (1991) Atmospheric aerosols: Global climatology and radiative characteristics. A. Deepak Pub., USA.

Dubovik, O., Smironov, A., Holben, B.N., King, M.D., Kaufman, Y.J., Eck, T.K., Slutsker, I. (2000) Accuracy assessments of aerosol optical properties retrieved from Aerosol Robotic Network (AERONET) Sun and sky radiance measurements. Journal of Geophysical Research 105, 9791-9806, doi:10.1029/2000JD900040.

Gordon, H.R., Wang, M. (1992) Surface-roughness considerations for atmospheric correction of oceans with SeaWiFS: A preliminary algorithm. Applied Optics 31, 4261-4267.

Hauser, A., Oesch, D., Wunderle, S. (2004) NOAA AVHRR derived Aerosol Optical Depth (AOD) over Land: A comparison with AERONET data. Optica Puray Aplicada 37, 3131-3135.

Herman, J.R., Celarier, E.A. (1997) Earth surface reflectivity climatology at 340-380 nm from TOMS data. Journal of Geophysical Research 102, 28003-28011, doi:10.1029/97JD02074.

Higurashi, A., Nakajima, T. (1999) Development of a two-channel aerosol retrieval algorithm on a global scale using NOAA AVHRR. Journal of the Atmospheric Sciences 56, 924-941.

Holben, B.N., Eck, T.F., Slutsker, I., Tanré, D., Buis, J.P., Stezer, A., Vermote, E., Reagan, Y., Kaufman, U.J., Nakajima, T., Lavenu, F., Jankpwiak, I., Smimov, A. (1998) AERONET-A federated instrument network and data archive for aerosol characterization. Remote Sensing of Environment 66, 1-16.

In, H.J., Kim, Y.P., Lee, K.H. (2008) Regional aerosol optical thickness distribution derived by CMAQ model in the siberian forest fire emission episode of May 2003 (Borrego, C. and Mirana, A.I. Eds), Air Pollution Modeling and Its Application XIX, Springer, 2,118-126, doi: 10.1007/978-1-4020-8453-9_13.

Jaffe, D., Berschi, I., Jaeglé, L., Novell, P., Reid, J.W., Tanimoto, H., Vingarzan, R., Westphal., D.L. (2004) Long-range transport of Siberian biomass burning emissions and impact on surface ozone in western North America. Geophysical Research Letters 31, L16106, doi:10.1029/2004GL020093.

Kaufman, Y.J., Tanré, D. (1992) Atmospherically resistant vegetation index (ARVI) for EOS-MODIS. IEEE Transactions on Geoscience and Remote Sensing 30, 261-270.

King, M.D., Kaufman, Y.J., Tanré, D., Nakajima, T. (1999) Remote sensing of tropospheric aerosols from space: Past, Presents, and Future. Bulletin of the American Meteorological Society 80, 2229-2259.

Lee, K.H., Kim, J.E., Kim, Y.J., von Hoyningen-Huene, W. (2005) Impact of the smoke aerosol from Russian forest fires on the atmospheric environment over Korea during May 2003. Atmospheric Environment 39, 85-99.

Miller, R.L., Tengen, I. (1998) Climate response to soil dust aerosols. Journal of Climate 11, 3247-3267.

Nakajima, T., Tanka, M. (1986) Matrix formulation for the transfer of solar radiation in a plane-parallel scattering atmosphere. Journal of Quantitative Spectroscopy and Radiative Transfer 35, 13-21.

Nakajima, T., Tanka, M. (1988) Algorithms for radiative intensity calculations in moderately thick atmospheres using a truncation approximation. Journal of Quantitative Spectroscopy and Radiative Transfer 40, 51-69.

Nakajima, T.Y., Murakami, H., Hori, M., Nakajima, T., Aoki, T., Oishi, T., Tanaka, A. (2003) Efficient use of an improved radiative transfer code to simulate near-global distributions of satellite-measured radiances. Applied Optics 42, 3460-3471.

Schwartz, S.E., Arnold, F., Blanchet, J.-P., Durkee, P.A., Hofmann, D.J., Hoppel, W.A., King, M.D., Lacis, A.A., Nakajima, T., Ogren, J.A., Toon, O.B., Wendisch, M. (1995) Group report: Connections between aerosol properties and forcing of climate (Charlson, R.J. and Heintzenberg, J. Eds), Aerosol Forcing of Climate, John Wiley and Sons, pp. 251-280.

Solomon, S., Qin, D., Manning, M., Chen, Z., Marquis, M., Averyt, K.B., Tignor, M., Miller, H.L. (2007) Contribution of Working Group I to the Fourth Assessment Report of the Intergovernmental Panel on Climate Change (IPCC). Cambridge University Press. USA, pp. 718-727.

Soufflet, V., Tanré, D., Royer, A., O'Neil, N.T. (1997) Remote sensing of aerosols over boreal forest and late water from AVHRR data. Remote Sensing of Environment 60, 22-34.

Torres, O., Bhartia, P.K., Herman, J.R., Ahmad, Z., Gleason, J. (1998) Derivation of aerosol properties from satellite measurements of backscattered ultraviolet radiation: Theoretical basis. Journal of Geophysical Research 103, 17099-17110, doi:10.1029/ 98JD00900.

Torres, O., Bhartia, P.K., Herman, J.R., Sinyuk, A., Ginoux, P., Holben, B. (2002) Along-term record of aerosol optical depth from TOMS observations and comparison to AERONET measurements. Journal of Atmospheric Sciences 59, 398-413.

Von Hoyningen-Huene, W., Freitag, M., Burrows, J.B. (2003) Retrieval of aerosol optical thickness over land surfaces from top-of-atmosphere radiance. Journal of Geophysical Research 108, 4260-4279, doi:10.1029/ 2001JD002018.

(Received 2 December 2010, accepted 23 March 2011)